*Tellus (1993), 45A, 270–280*
*Printed in Belgium – all rights reserved*


TELLUS
*ISSN 0280–6495*

# A method to determine the theoretical maximum error growth in atmospheric models

By BERNARD URBAN, *Direction de la Météorologie Nationale, CNRM/GMAP, 42, avenue Coriolis, 31057 Toulouse, France*

(Manuscript received 19 March 1992; in final form 15 March 1993)

ABSTRACT

For a fixed forecast range and initial state of an atmospheric model, we present a practical method to determine the error of this initial state which maximizes the ratio of final to initial error. The method uses the adjoint model concept. Numerical results for a simple barotropic model are given. We show on a sample of real cases that there is a negative correlation between the above ratio and a least square forecast skill. We discuss this result and the use of the method for a priori estimation of the quality of numerical forecasts.

## 1. Introduction

For the last 20 years, substantial improvements have been accomplished in numerical weather forecasts. Nevertheless, the variability in the skill of these predictions is still large.

When we look at the reasons of the forecast skill variability, we can find two kinds of errors: (i) the model dynamics and physics do not correspond to reality, (ii) the initial state of the model is not known exactly.

The type (i) error will certainly be reduced in the near future as the constantly increasing available computer power makes it possible to use more refined dynamics and physics. For type (ii) errors, the improvements are ultimately limited by the observational network. Today, there is a trend to replace ground-based observation facilities by large amount of satellite data, which appear to have less detailed information. The use of a sophisticated assimilation scheme will help only to a certain point to improve the quality of the initial state.

For all these reasons, it appears that the error in the initial state of a model will be more and more important to explain the skill of the model. This fact gave rise to a probabilistic approach of the problem of the forecast (Epstein, 1969): we do no longer follow the evolution of a point in the phase space of the model, but we are interested in the behaviour in time of a cloud of points centered around the "best" estimate of the atmospheric state. The final dispersion of this cloud gives then information about the quality of the forecast.

The only numerically tractable method to handle such a probability distribution is the well-known Monte-Carlo method. There are two serious difficulties associated with it.

- *The initial error distribution.* A variety of direct perturbation methods to obtain such a distribution can be found (see for instance Baumhefner, 1988). The lagged-average method takes as a sample of such an error distribution a set of forecasts slightly different in their starting time (Hoffman and Kalnay, 1983; Brankovic and al., 1988). But it is uncertain that all these methods give a sample compatible with the initial error distribution.
- *The size of the sample to be used.* It has been shown that for simple turbulence models the size may be as small as 10 (Leith, 1974). But this is perhaps not true for meteorological models with physical parameterizations. So the numerical cost of the Monte-Carlo method is at least 10 times the cost of a simple model integration.

Recently (Lacarra and Talagrand, 1988; Farrell, 1989; Vukicevic, 1991) proposed an alternative to Monte-Carlo: they compute the initial error which gives rise to the worst forecast. To do so, they determine the biggest ratio of final to initial error (this scaling must be introduced if we don't want to obtain as solution an infinite final error). As noted in Lacarra and Talagrand (1988), this problem can be reduced to an eigenvalue problem. The numerical cost of such a method is prohibitive for a realistic model, if more than the highest eigenvalues is wanted. In this paper, we present an algorithm to determine at low cost these eigenvalues. This method is similar to the one suggested in Lorenz (1965).

We first recall the general theory of the method. Secondly, we use it to treat the simple case of a barotropic non-divergent model. A powerful numerical method is then introduced (the Lanczos algorithm) which allows a crucial numerical simplification of the computation. Finally, we show the utility of our method for a priori quality estimation by the comparison of:

- the maximum ratio of final to initial error;
- several error scores defined from the difference between the forecast and the corresponding "truth".

## 2. Theory

In the following, the state of the atmosphere is represented by a point $x$ in a phase space $E$. The evolution of the atmosphere can be described by:

$$\frac{dx}{dt} = B(x). \tag{1}$$

Here $E$ and the operator $B$ depends on the atmospheric model used. The system (1) will be replaced for numerical integration by: $y_n = A(y_0, n)$, where $y_i$ will be a vector of a $N$-dimensional space $F$, and represents the state of the atmosphere at time $i\,\Delta t$, $\Delta t$ being the time step of the discretization.

For instance, a vector of $F$ will have for components grid point values or spectral coefficients of the meteorological fields. We will denote by $\langle \cdot, \cdot \rangle$ the inner product in $F$. The initial state $y_0$ of the atmosphere is obtained through an analysis-initialisation scheme. We will call $z_0$ the "true" initial state, which gives the best forecast.

We will also define a differentiable functional $\mathcal{J}$ (the cost function) which measures the discrepancy between $y_n$ and $z_n = A(z_0, n)$. The ratio $Q$ we want to maximize to obtain the worst case of prediction error is then:

$$\frac{\mathcal{J}(y_n - z_n)}{\mathcal{J}(y_0 - z_0)} = Q.$$

We will denote: $e_i = y_i - z_i$ and we notice that: $e_n = A(z_0 + e_0, n) - A(z_0, n) = H(e_0)$ which defines the operator $H$. Thus, $Q$ is a function of $e_0$ only, which we want to maximize:

$$Q(e_0) = \frac{\mathcal{J}(H(e_0))}{\mathcal{J}(e_0)}. \tag{2}$$

A necessary condition for maximizing $Q$ is: $\nabla|_{e_0} Q = 0$, where $\nabla|_{e_0}$ represents the gradient operator taken at point $e_0$. The differentiation of (2) leads to:

$$\nabla|_{e_0} Q = \frac{-(\nabla|_{e_0} \mathcal{J})\,\mathcal{J}(e_n) + H'^*(\nabla|_{He_0} \mathcal{J})\,\mathcal{J}(e_0)}{\mathcal{J}^2(e_0)},$$

where $H'^*$ is the adjoint* of the linear operator $H'$, which is the differential at $e_0$ of $H$:

$$H' = DH|_{e_0} = DA(\cdot, n)|_{y_0}.$$

We will choose $\mathcal{J}(e_0) = \langle e_0, e_0 \rangle$ which seems one of the simplest possible choise, so: $\nabla|_{e_0} \mathcal{J} = 2e_0$ and the necessary condition for $Q(e_0)$ to be a maximum becomes:

$$\nabla|_{e_0} Q = 0 \Leftrightarrow -2e_0 \mathcal{J}(e_n) + H'^* 2H(e_0)\,\mathcal{J}(e_0) = 0$$

and then:

$$\nabla|_{e_0} Q = 0 \Leftrightarrow e_0 Q(e_0) = H'^* H(e_0). \tag{3}$$

The determination of the maximum of $Q$ (or minimum of $-Q$) will need the use of minimiza-

* The adjoint of a linear operator $A: E \to F$ is the unique linear operator $A^*: F \to E$ verifying: $\langle A^* x, y \rangle_E = \langle x, Ay \rangle_F$ for all $x \in F$ and $y \in E$. Here $\langle \cdot, \cdot \rangle_E$ is the inner product of space $E$ and $\langle \cdot, \cdot \rangle_F$ is the inner product of space $F$, so $A^*$ depends on the choice of both scalar products.

tion algorithms. They use the vector $\nabla Q$, and so need the calculation of $H$, $\mathcal{J}$, $\nabla\mathcal{J}$, and $H'^*$. Notice that the choice of $\langle \cdot, \cdot \rangle$ and $\mathcal{J}$ will determine $\nabla\mathcal{J}$ and $H'^*$.

The expression (3) gives an interesting case if $H$ is linear (that implies: $H' = H$): the maximum of $Q$ is the biggest eigenvalue of the symmetric linear operator $H'^*H$, and the value for which it is reached is the associated eigenvector. A huge simplification in the numerical problems can then occur under the assumption of linearity, because eigenvalue problems are much less expensive to solve than minimization problems. In the next parts, we will take advantage of this remark to obtain a numerically tractable problem.

## 3. The barotropic model

We now apply the results of the first part to the barotropic non-divergent model:

$$\frac{\mathrm{d}y}{\mathrm{d}t} = L^{-1}J(y, -Ly + f),$$

where $y$ is the streamfunction on the sphere, $J(\cdot, \cdot)$ the jacobian on the sphere, $L$ an elliptic operator: $L = -\Delta + 1/R^2$, with $\Delta$ the laplacian and $R$ the radius of deformation ($R = 2000$ km in our model).

We recall that: $f = 2\Omega \sin\theta + f_0 h_b/D$ where:

- $D$ is the atmospheric vertical scale ($D = 10$ km),
- $f_0$ a mean Coriolis parameter,
- $\Omega$ is the earth vorticity,
- $\theta$ is the latitude,
- $h_b$ the earth surface height.

The phase space $E$ will be the space of real funcions defined on the sphere $S$ which are differentiable. The inner product will be:

$$\langle a, b \rangle = \int_S (\nabla a \cdot \nabla b + ab/R^2)\, \mathrm{d}s.$$

The choice of this inner product has a physical meaning: $\langle y, y \rangle$ is the sum of the kinetic energy and of the potential energy of the state defined by the streamfuncion $y$ (see Legras and Ghil, 1983). Thus, this total energy is constant in time for our model.

The discrete model will be a spectral model with triangular truncation. We denote by $p$ the projection of $E$ on the subspace $F$ corresponding to this trunction. The time discretization will be a leap-frog one. It does not conserve energy, but the variations are less than 1 % for the forecast range we will use (less than 4 days).

If $\Delta t$ is the time step used and $B = L^{-1}J(\cdot, -L(\cdot) + f)$, we have:

$$y_{n+1} = A(y_0, n+1) = q \underbrace{\begin{pmatrix} 2\Delta t p B(\cdot) & I \\ I & 0 \end{pmatrix}}_{G} \begin{pmatrix} y_n \\ y_{n-1} \end{pmatrix}, \qquad n > 0,$$

where $q$ is a projection operator: $q(x, y) = x$ and $I$ is the identity matrix. We define function $i$ as: $i(x) = (x, x)$ for $x$ belonging to $F$. Then:

$$y_n = A(y_0, n) = qG^{n-1} \underbrace{\begin{pmatrix} \Delta t p B(\cdot) & I \\ I & 0 \end{pmatrix}}_{\tilde{G}} i(y_0), \qquad n > 0,$$

where $\tilde{G}$ corresponds to the first time step of the model.

From the first part we recall that:

$$H' = DA(\cdot, n)|_{y_0} = qDG|_{(y_{n-1}, y_{n-2})} \cdots DG|_{(y_1, y_2)}\, D\tilde{G}|_{(y_0, y_0)}\, i,$$

and:

$$H'^* = i^* D\tilde{G}^*|_{(y_0, y_0)} \cdots DG^*|_{(y_{n-1}, y_{n-2})}\, q^*,$$

where it can be shown easily that: $i^*(x, y) = x + y$ and $q^*(x) = (x, 0)$ for all inner products.

The other factors are explicitly:

$$DG|_{(x,y)} = \begin{pmatrix} 2\Delta t\, pDB|_x(\cdot) & I \\ I & 0 \end{pmatrix},$$

$$DG^*|_{(x,y)} = \begin{pmatrix} 2\Delta t\, pDB^*|_x(\cdot) & I \\ I & 0 \end{pmatrix}.$$

We can derive also:

$$DB|_y = L^{-1}(J(\cdot, -Ly+f) - J(y, L(\cdot))),$$

$$DB^*|_y = -L^{-1}(J(\cdot, -Ly+f) - LJ(y, \cdot)).$$

All these calculations were made with the space $F \times F$ having the canonical inner product originating from $F$, and depend heavily on this inner product.

It is important to notice that in the previous calculations of $H'$ and $H'^*$, we have actually linearized about the model trajectory originating from $y_0$, and not about the model basic state $y_0$. The two approaches are identical only if $y_0$ is a stationary solution for the model, of if we are interested in instantaneous error growing rates. A lot of the non-linear dynamics of the model can then be taken into account. For more details about the linearization around a basic state, see Farrell (1989). Our method is also different from Liapunov exponents computations, which give information on the vary long term behaviour of the model.

Numerical experiments show that for a forecast range of less than 4 days and $\langle e_0, e_0 \rangle^{1/2}$ values being less than 1 % of $\langle y_0, y_0 \rangle^{1/2}$, the discrepancy between $H$ and $H'$ is less than 0.1 %. Similar tests of linearity were performed successfully in Lacarra and Talagrand (1988) for a barotropic model and in Vukicevic (1991) for a limited area model.

This means that we can work with the hypothesis that $H$ is linear under the above-mentioned conditions. We have shown in part 1 that this reduces our minimization problem of $Q$ to an eigenvalue problem. But since for a T13 truncation the matrix $H'^*H$ involves $192 \times 192$ elements, the calculation of $H'^*H$ for a 2 day forecast range will take $2 \times 192$ days of evolution of the model. We see on this example that the direct calculation of $H'^*H$ is not possible for realistic models with millions of degrees of freedom.

What we need is a method for the calculation of the eigenvalues and eigenvectors of $H'^*H$ without handling the corresponding matrix. This is possible with the Lanczos algorithm: it needs only the knowledge of an operator which compute $H'^*H(x)$ for a given vector $x$. It is fully described in Parlett (1978); a summary is presented in the Appendix.

## 4. Results for the barotropic model

We present first the typical results of our method for a real case. We have chosen the 21 November 1990, all experiments starting at 00 UTC and having a forecast range of two days. The stream function fields are plotted in cylindrical projection. We present the initial field (Fig. 1), the first four eigenvectors at truncation T21 (Figs. 2–5) and

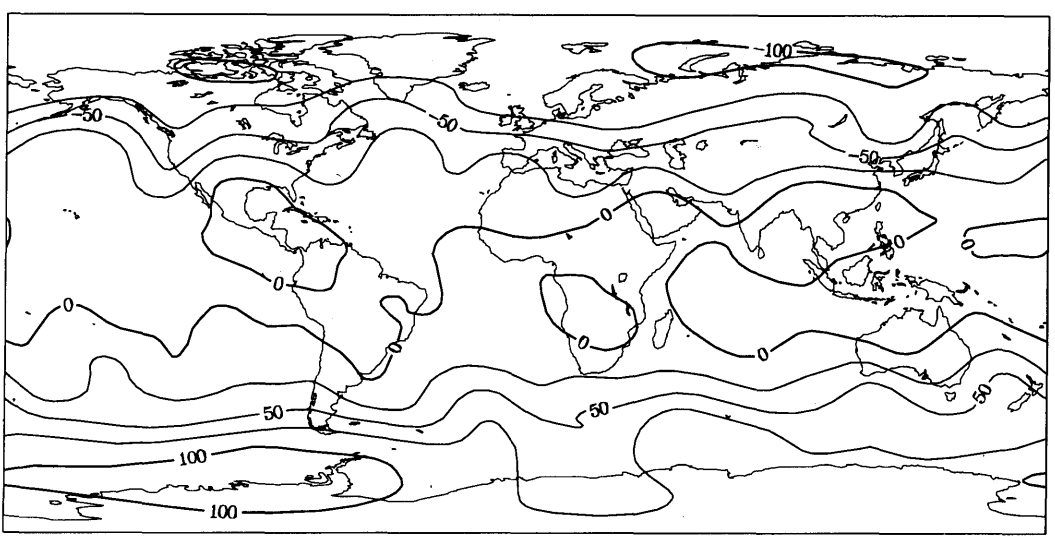


*Fig. 1.* Initial state for 00 UTC 21 Nov. 1990; stream function at 500 hPa scaled by $10^{-6}$.

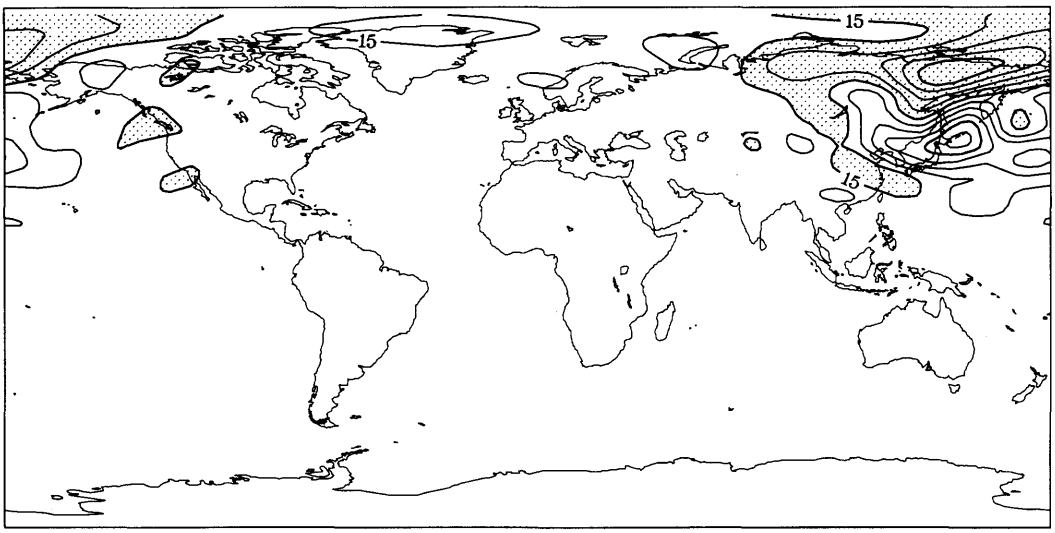


*Fig. 2.* Eigenvector 1 of $H^*H$ for 00 UTC 21 Nov. 1990 at truncation T21 and forecast range 48 h; eigenvalue: 35.20. The field has been scaled by 100, and the shaded areas are for positive values above 15.

the first three eigenvectors at truncation T33 (Figs. 6–8).

With the application of the Lanczos algorithm, we can compute several eigenvalues with a high precision (the scalar products of our eigenvectors have an absolute deviation from their theoretical value less than $10^{-6}$; the quantities $\langle H'^*Hy - \beta y, H'^*Hy - \beta y \rangle^{1/2}$ are less than $10^{-2}$, where $y$ and $\beta$ are associated eigenvector (normalised) and eigenvalue). The possibility to obtain several eigenvectors is a big advantage of the Lanczos method; with the more classical power method algorithm used in Vukicevic (1991), we can obtain only the first eigenvector.

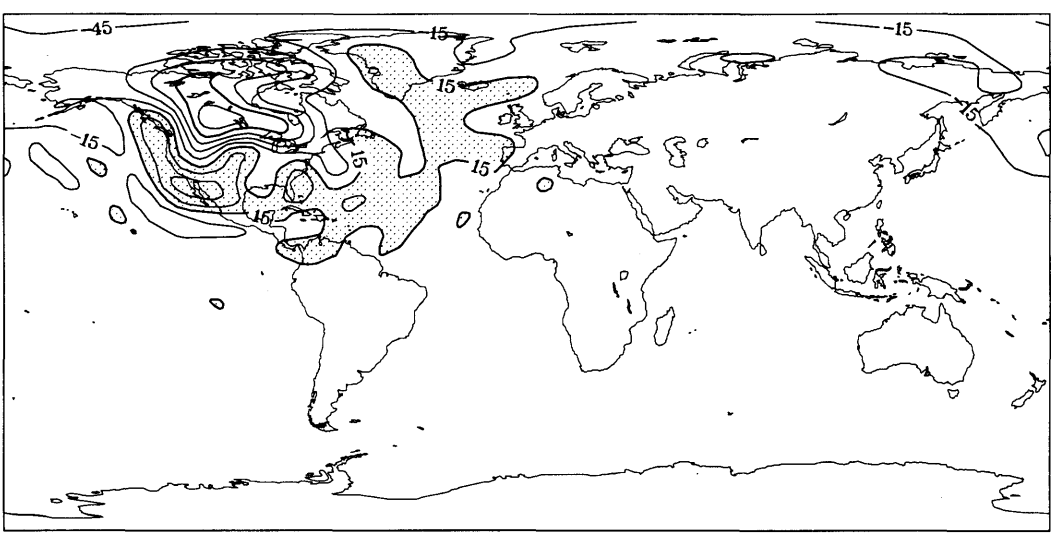


*Fig. 3.* Eigenvector 2 of $H^*H$ for 00 UTC 21 Nov. 1990 at truncation T21 and forecast range 48 h; eigenvalue: 21.74. The field has been scaled by 100, and the shaded areas are for positive values above 15.

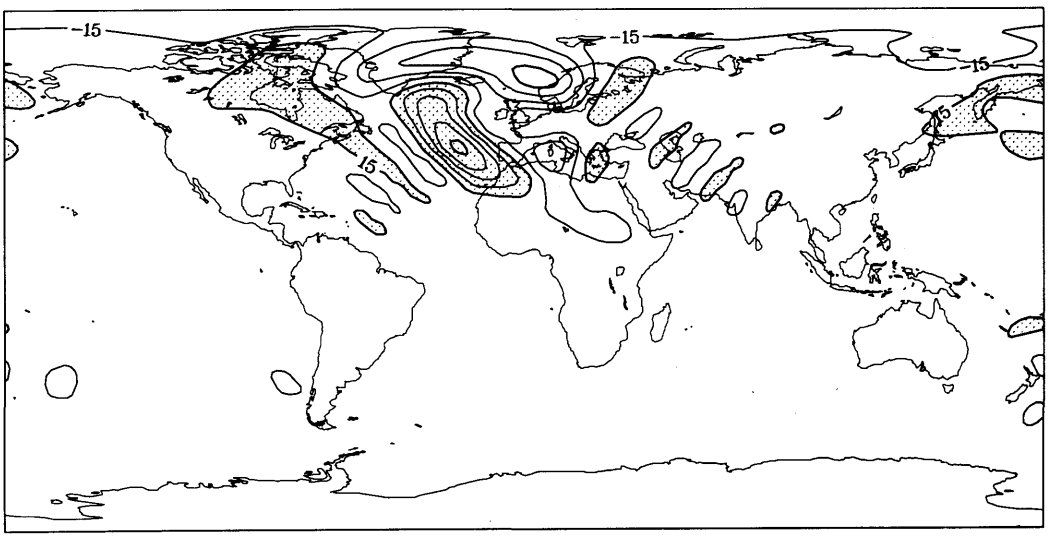


*Fig. 4.* Eigenvector 3 of $H^*H$ for 00 UTC 21 Nov. 1990 at truncation T21 and forecast range 48 h; eigenvalue: 16.7. The field has been scaled by 100, and the shaded areas are for positive values above 15.

We can distinguish for the eigenvector fields two kinds of extreme patterns:

- a dipole pattern, with a high maximum near to a very low minimum, the rest of the field being close to 0. See for example Figs. 2, 3 or 6;
- a wave pattern, with a succession of maxima and minima, oriented eastwest. See for example Figs. 5 or 7.

These above-mentioned distinct behaviors are quite general, but most often the patterns are intermediate and noisy. We can notice that the

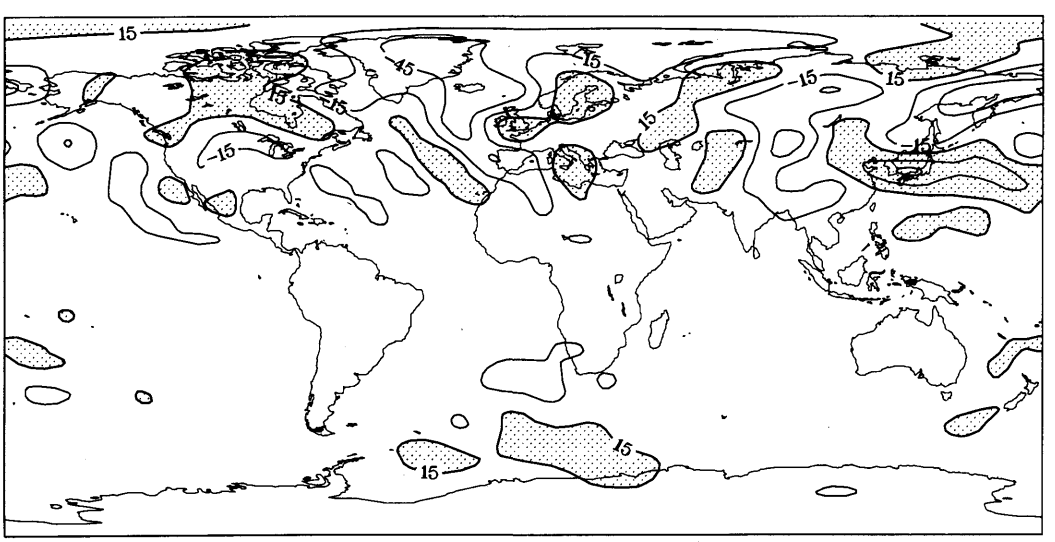


*Fig. 5.* Eigenvector 4 of $H^*H$ for 00 UTC 21 Nov. 1990 at truncation T21 and forecast range 48 h; eigenvalue: 15.46. The field has been scaled by 100, and the shaded areas are for positive values above 15.

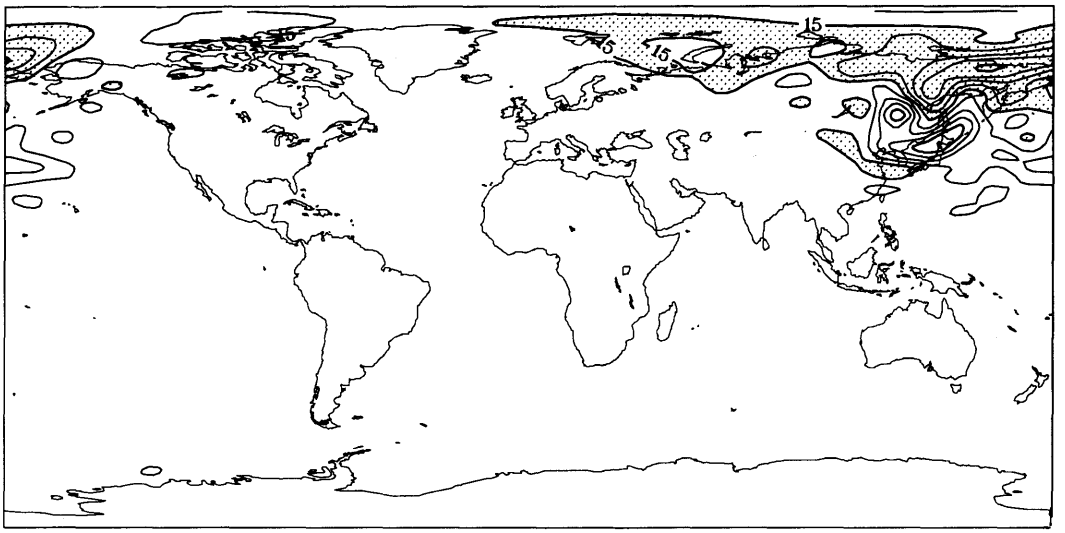


*Fig. 6.* Eigenvector 1 of $H^*H$ for 00 UTC 21 Nov. 1990 at truncation T33 and forecast range 48 h; eigenvalue: 71.69. The field has been scaled by 100, and the shaded areas are for positive values above 15.

southern hemisphere exhibits very often a quasi-uniform field. This is also true for summer situations. There is also an important influence of the truncation on the results (forecast range being fixed): the largest eigenvalues at truncation T21 are typically 4 times bigger than these for T13; those at T33 are 2 times bigger than for T21. The eigenvectors patterns of same rank (or of very close rank) show a tendency to converge as the truncation increases. This is visible between Figs. 2 and 6 (vectors of rank 1), and at a least extent between Figs. 5 and 8 (vector of rank 4 at T21 and of rank 3 for T33).

We will now test the usefulness of the method

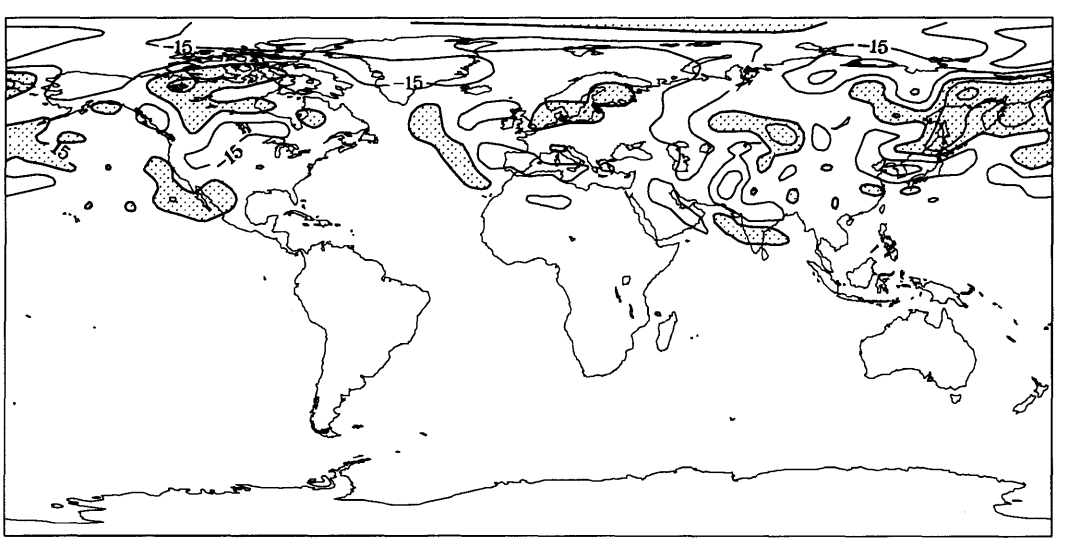


*Fig. 7.* Eigenvector 2 of $H^*H$ for 00 UTC 21 Nov. 1990 at truncation T33 and forecast range 48 h.; eigenvalue: 44.9. The field has been scaled by 100, and the shaded areas are for positive values above 15.


*Fig. 8.* Eigenvector 3 of $H^*H$ for 00 UTC 21 Nov. 1990 at truncation T33 and forecast range 48 h; eigenvalue: 43.55. The field has been scaled by 100, and the shaded areas are for positive values above 15.

described above. For this, we will try to see if some skill of a sophisticated model has a link with the highest eigenvalue we have computed.

We will choose the global French model EMERAUDE as the sophisticated one. The skill will be some weighted spectral mean quadratic difference between EMERAUDE's forecast and the corresponding analysis, taken as the reality $z_n$. In computing this difference, we have truncated EMERAUDE's fields to the spectral resolution of the barotropic model, so this skill is a large scale one. The weights for our quadratic differences are of two types:

- All weights are equal. This means that we take for the error an euclidean scalar product in the spectral space.
- The weights are proportional to the power-3 of the global wavenumber for a given spectral coefficient. So we give more importance to large scale errors. For internal consistency, the scalar product used for the adjoint computation in the barotropic model is also modified in the same manner. We recall that this leads to an another adjoint than in the previous case.

The results are shown for spectral truncation T21 (48-h forecast) in the Figs. 9, 10, where we have plotted the points of coordinates (highest eigenvalue, error) for our sample of size 23. The period taken for our sample is covering November 1990 to January 1991. We always kept an interval of 2 days between the forecast date of one case and the starting point of the following case. This was done to eliminate statistical dependencies in the sample.

There seems to be an alignment of the points, showing that high errors correspond to low eigenvalues. At first, this seems not natural: we would expect a correlation high eigenvalues - high errors (low quality). A more precise study shows that high eigenvalues are mostly related with blocking situations. In such cases, EMERAUDE maintains the blocking to a certain extent and has so a low forecast error. The fact that the barotropic model exhibits high maximum eigenvalues during blocking instead of low ones is probably caused by the coarse simulations we can only obtain with such a model, which does not treat baroclinic instability and diabatic effects. There is no doubt than doing the same experiments with a better model will show a different behaviour.

For all cases, we can notice that the dispersion of the points is larger when the predictor is low. The above alignment is not visible for truncation T13 and for a 24-h forecast range.

The cloud of points shown above is too large to

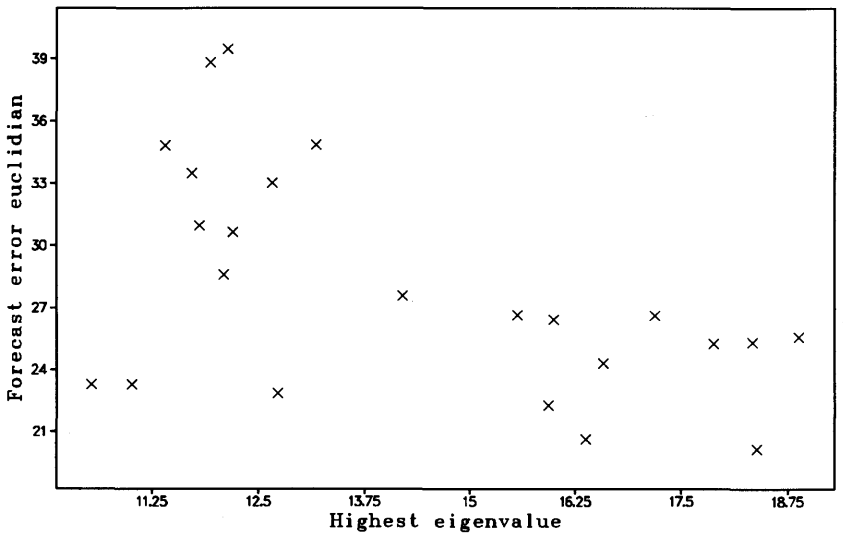


*Fig. 9.* Plotting of the points of coordinates (highest eigenvalue, EMERAUDE euclidean forecast error). Eigenvalues were obtained for a 48 h forecast of the barotropic model at truncation T21.

conclude anything by looking at the picture. As done in Palmer and Tibaldi (1988), who present statistical regressions between predictors taken from previous forecasts and a forecast skill, we need to compute such a regression for our cloud of points. To do so, we have measured the correlation between our two quantities with the correlation test from Spearman (which does not make any gaussian assumption). A description of this test can be found in Kendall and Stuart (1979) and a

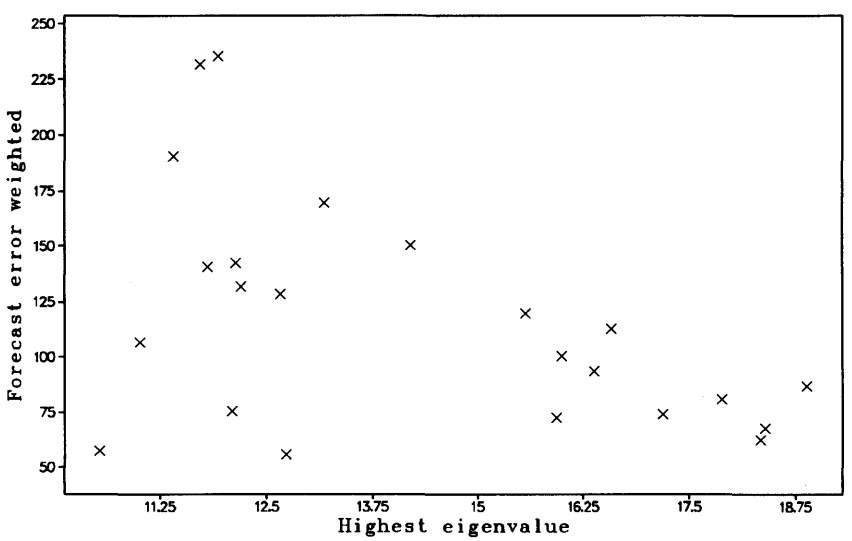


*Fig. 10.* Plotting of the points of coordinates (highest eigenvalue, EMERAUDE weighted forecast error). Eigenvalues were obtained for a 48-h forecast of the barotropic model at truncation T21.

Table 1. *Correlation between highest eigenvalue and forecast skill*

| Scalar product | Regression coeff. | T13 24-h forecast | T21 48-h forecast |
|---|---|---|---|
| Euclidian | linear | 0.038 | −0.470 |
| | Spearman | −0.183 | −0.603 |
| Weighted | linear | 0.057 | −0.492 |
| | Spearman | −0.19 | −0.566 |

table of critical values is available in Siegel (1959). For information, the classical linear regression coefficient was also calculated.

To interpret the table above, the significance level at 5% for the Spearman test is:

- $\approx 0.351$ for a sample of size $n = 23$;
- $\approx 0.312$ for a sample of size $n = 29$ (case T13 and 24-h forecast range).

The absolute value of the coefficient computed in the tables must be higher than these critical values to conclude that with an error less than 5%, our sample is not chosen by random. A negative correlation in the table show that high predictor values are correlated with low errors. As we can see, the T21 case shows clearly a significant negative correlation between the highest eigenvalues and the EMERAUDE large scale forecast errors.

## 5. Conclusion

We have presented a method to calculate the maximum error growth of the initial state error for a numerical atmospheric model working at a fixed forecast range. Because this range is less than 4 days, a huge numerical simplification of the initial variational problem is possible. The simplified problem is equivalent to a symmetric eigenvalue research. The highest eigenvalue of the problem is equal to the maximum error growth we were looking for; and the corresponding eigenvector is the initial error field which achieves this maximum error growth. The use of the Lanczos algorithm makes it numerically feasable to compute the above quantities, even for complicated atmospheric models, if their adjoint is available.

This method was used on a simple model, and we tried to detect if the eigenvalues we found can be used as predictors for determining the a priori forecast quality of a more sophisticated model. We found a significant negative correlation between these two quantities for a resolution of T21, and for global forecast quality definitions. Regional applications (as studied in Barkmeijer (1992)) will be the most useful in practice. The method can also treat this case with modified forecast quality concepts, having heavy weights on particular geographic locations.

As soon as an operational model will be designed with a built-in adjoint (as is planned at ECMWF and Météo-France), much better results can be expected to predict by this method the quality of the forecast itself.

## 6. Acknowledgments

The start of this work has been made possible with the help of P. Bernardet.

## 7. Appendix

*The Lanczos algorithm*

The Lanczos algorithm searches the eigenvalues and eigenvectors of a *symmetric* linear operator $A$ in the space $R^n$. For $i$ in the following interval: $1 \leqslant i \leqslant n$, we note $\lambda_i$ the $i$th eigenvalue of $A$ and $x_i$ the corresponding eigenvector; the eigenvalues are sorted by increasing value: $\lambda_i \leqslant \lambda_j$ if $i \leqslant j$. The idea is based on the convergence for a randomly choosen $x$ of $A^m(x)$ toward $\lambda_n x_n$, when $m \to \infty$. We have the following lemmas.

**Lemma 1**. For $i > 0$, we note $K^i(r_0)$ the subspace generated by

$$(r_0, A(r_0), ..., A^{i-1}(r_0)).$$

It is possible to find an orthonormal base of $K^i(r_0)$ noted $(q_1, q_2, ..., q_i)$, so that $\forall j \in ]1, i[$,

$(q_1, q_2, ..., q_j)$ is an orthonormal base of $K^j(r_0)$. The algorithm giving the $q_i$ is:

- To start $(i=0)$:

$q_0 = 0$; choose $r_0 \neq 0$; $\beta_0 = |r_0|$.

- For $i > 0$:

$$q_i = \frac{r_{i-1}}{\beta_{i-1}}; \qquad r_i = Aq_i - q_i\langle q_i, Aq_i\rangle - q_{i-1}\beta_{i-1}; \qquad \beta_i = |r_i|.$$

**Lemma 2.** The linear operator $A_i$ defined on $K^i(r_0)$ by: $A_i(x) = A(x)$ for $x \in K^i(r_0)$ has a tridiagonal matrix in the base $(q_1, q_2, ..., q_i)$ of $K^i(r_0)$ defined in Lemma 1. The diagonal elements are $\alpha_i = \langle q_i, Aq_i\rangle$ for $i > 0$ and the elements of the second diagonal are $\beta_i$ for $i > 0$.

It is numerically cheap to compute the eigenvalues and eigenvectors of a tridiagonal matrix. The main result demonstrated in Parlett (1978) is that the eigenvalues and eigenvectors of $A_i$ are converging rapidly to those of $A$ as $i \to n$, especially the eigenvalues at the end of the spectrum of $A$. The Lanczos algorithm then simply computes the $i$ eigenvalues of the tridiagonal matrix in lemma 2 for $i$ increasing from 1 to $n_0 \leqslant n$ and by going back to the base of reference of $R^n$, we find approximate eigenvectors of $A$ (we need for this to keep $(q_1, q_2, ..., q_i)$ in memory). In Parlett (1978), a condition on the $\beta_i$ is given which indicates when to stop the algorithm when a choosen precision on the eigenvectors at the end of the spectrum of $A$ is obtained. For our practical experiments, we found for a truncation of T21 that the 4 biggest eigenvalues were computed with 2 significant digits at least with $n_0 \approx 30$ iterations (to compare with the dimension of $R^n$: $n = 484$).

## REFERENCES


Baumhefner, D. P. 1988. Forecast skill and predictability at the extended range using Monte-Carlo ensemble integrations from a general circulation model. *ECMWF Workshop 'Predictability in the medium and extended range'*, 16-18 May 1988, pp. 25–44.

Barkmeijer, J. 1992. Local error growth in a barotropic model. *Tellus 44A*, 314–323.

Brankovic, C., Molteni, F., Palmer, T. N., Tibaldi, S., and Cubasch, U. 1988. Extended range ensemble forecasting. *ECMWF Workshop 'Predictability in the medium and extended range'*, 16–18 May 1988, pp. 45–88.

Epstein, E. S. 1969. Stochastic dynamic prediction. *Tellus 21*, 739–757.

Farrell, B. F. 1989. Optimal excitation of baroclinic waves. *J. Atmos. Sci. 46*, 1193–1206.

Hoffman, R. N., and Kalnay, E. 1983. Lagged average forecast. *Tellus 35A*, 100–118.

Kendall, M. and Stuart, A. 1979. *The advanced theory of statistics*, vol. 2, 4th edition. Charles Griffin & Co Ltd., London, 503–505.

Lacarra, J.-F., and Talagrand, O. 1988. Short range evolution of small perturbations in a barotropic model. *Tellus 40A*, 81–95.

Leith, C. E. 1974. Theoretical skill of Monte-Carlo forecasts. *Mon. Wea. Rev. 102*, 408–418.

Legras, B., and Ghil, M. 1983. Ecoulements atmosphériques stationnaires, périodiques et apériodiques. *J. Mécanique théorique appliquée, special issue 1983*, 45–82.

Lorenz, E. N. 1965. A study of the predictability of a 28-variable atmospheric model. *Tellus 17*, 321–333.

Palmer, T. N., and Tibaldi, S. 1988. On the prediction of forecast skill. *Mon. Wea. Rev. 116*, 2453–2480.

Parlett, B. N. 1978. *The symmetric eigenvalue problem.* Academic Press, New York, 343.

Siegel, S. 1959. *Non parametric statistics for behavioral sciences.* Mac Graw-Hill, International Student Edition, New York, 284.

Vukicevic, T. 1991. Skill forecast based on the finite-time unstable linear modes for a primitive equation regional forecast model. *NCAR Internal Note 0501/92-1*, November 1991.